SKB

Impact of H$_2$ and Ar on the production of corrosive species in vapour exposed to gamma irradiation in canisters for spent nuclear fuel

Mats Jonsson

SVENSK KÄRNBRÄNSLEHANTERING

Impact of H₂ and Ar on the production of corrosive species in vapour exposed to gamma irradiation in canisters for spent nuclear fuel

Mats Jonsson, Applied Physical Chemistry, KTH

Abstract

In this study the oxidant production in the gamma irradiated water vapor present in a sealed canister for spent nuclear fuel has been elucidated on the basis of numerical simulations. The impact of H_2 produced from anoxic corrosion of iron as well as the impact Ar present in the canister have also been investigated. The results of the simulations show that H_2 efficiently suppresses the radiolytic production of oxidants. Furthermore, the simulations indicate that the presence of Ar may have a significant effect on the radiolysis of water vapor, especially for low amounts of water in the canister.

Sammanfattning

I denna studie har produktionen av oxidanter i gammabestrålad vattenånga i en tillsluten kapsel för utbränt kärnbränsle utvärderats med hjälp av numeriska simuleringar. Effekten av H_2 som bildas vid anaerob korrosion av järn samt effekten av Ar som finns i kapseln har också studerats. Resultaten av simuleringarna visar att H_2 effektivt motverkar den radiolytiska bildningen av oxidanter. Simuleringarna indikerar också att närvaron av Ar kan ha en signifikant effekt på radiolysen av vattenånga, särskilt när mängden vatten i kapseln är liten.

Contents

1   Background

Upon sealing a copper-coated canister (of KBS-3 type) containing spent nuclear fuel, up to 600 g of water could be incorporated. Since the temperature in the canister will be high (140 °C), the water content will be fully vaporized in the empty volume of ca 1 m^3 (SKB 2010). Due to the intense flux of ionizing radiation inside the canister, the water vapor will undergo radiolysis producing both oxidizing and reducing species. The oxidizing products (mainly O_2 and H_2O_2) can corrode the canister material from the inside and thereby influence the long-term integrity of the canister.

In the absence of other oxidants, water vapor may corrode the iron in the canister. In this process, molecular hydrogen (H_2) is produced. It is well known that the presence of H_2 has a significant impact on the radiolysis of liquid water as it reduces the yield of oxidative radiolysis products (Pastina and LaVerne 2001, Trummer and Jonsson 2010). The purpose of the short project presented in this report is to assess the impact of H_2 on the radiolytic production of oxidants in water vapor on the basis of numerical simulations of the reaction system. In addition, the impact of Ar (which is the gas originally present in the sealed canister) and different relevant amounts (6.7, 244 and 600 g per canister) of water[1] are addressed.

---

[1] **Spahiu K, 2020.** Residual water in a KBS-3 canister and its effect on post-closure safety. SKBdoc 1914189 ver 1.0, Svensk Kärnbränslehantering AB. (Internal document.)

2 Radiation chemistry of water vapor

The radiation chemistry of water vapor was studied quite extensively around 50 years ago (Dixon 1970, Willis and Boyd 1976). In water vapor the charged species formed in the primary ionization processes following the absorption of ionizing radiation are not stabilized by solvation as in liquid water. Therefore, they will rapidly be converted to neutral species via neutralization reactions (mainly $e^- + H_3O^+ \rightarrow H + H_2O$). The radiation chemical yields for radiolysis of water vapor corresponding to ionic processes, neutral excitation and after charge neutralization are listed in Table 2-1. The G-value after charge neutralization is calculated from the G-values of the ionic process, the neutral excitation and the charge neutralization process (i.e., $H_3O^+ + e^- \rightarrow H^\bullet + H_2O$). For the hydrogen atom the G-value after charge neutralization is calculated as G(e^- ionic processes) + G($H^\bullet$ ionic process) + G($H^\bullet$ neutral excitation).

Table 2-1. Radiation chemical yields for radiolysis of water vapor (molecules/100 eV) (Willis and Boyd 1976).

Species	G (ionic processes)	G (neutral excitation)	G (after charge neutralization)
e^-	3.3	-	-
H_3O^+	3.3	-	-
OH	2.73	3.58	6.31
H	0.57	3.58	7.45
O	0.63	0.45	1.08
H_2	0.06	0.45	0.51

The reactions following radiolysis of water vapor are listed in Table 2-2. The rate constants are given in the unit cm^3 molecule^{-1} s^{-1} which is the unit commonly used for gas phase reactions. In a few cases the reactions follow third order kinetics (three body collisions) where one of the reactants is water itself. Assuming that the concentration of water will remain constant in the canister, the third order rate constants can be converted to operational second order rate constants. It should be noted that these rate constants are only valid at this specific water content. Table 2-2 also includes rate constants converted to operational second order rate constants and all other second order rate constants converted to the unit M^{-1} s^{-1} which is the format used in the numerical simulations.

Table 2-2. Reactions following radiolysis of water vapor (Willis and Boyd 1976).

Reactants	Product (s)	Rate const. cm^3 molecule^{-1} s^{-1}	Rate const. (converted) M^{-1} s^{-1}
H + H (+ H_2O)	H_2 (+ H_2O)	$2.00 \times 10^{-32*}$	2.41×10^8
H + OH (+ H_2O)	H_2O (+ H_2O)	$1.00 \times 10^{-30*}$	1.21×10^{10}
OH + OH (+ H_2O)	H_2O_2 (+ H_2O)	$1.00 \times 10^{-31*}$	1.21×10^9
O + OH	O_2 + H	5.00×10^{-11}	3.01×10^{10}
H + O_2 (+ H_2O)	HO_2 (+ H_2O)	$4.00 \times 10^{-31*}$	4.83×10^9
H + HO_2	H_2 + O_2	1.00×10^{-11}	6.02×10^9
H + HO_2	H_2O + O	1.00×10^{-21}	6.02×10^{-1}
H + HO_2	OH + OH	2.00×10^{-12}	1.20×10^9
HO_2 + HO_2	H_2O_2 + O_2	3.60×10^{-12}	2.17×10^9
H + O (+ H_2O)	OH (+ H_2O)	$2.50 \times 10^{-32*}$	3.02×10^8
H + H_2O_2	H_2O + O_2	1.00×10^{-13}	6.02×10^7
OH + H_2O_2	H_2O + HO_2	2.00×10^{-12}	1.20×10^9
OH + H_2	H_2O + H	9.00×10^{-14}	5.42×10^7
OH + OH	H_2O + O	2.30×10^{-12}	1.38×10^9
O + O (+ H_2O)	O_2 (+ H_2O)	$2.70 \times 10^{-33*}$	3.26×10^7
O + H_2	H + OH	3.00×10^{-16}	1.81×10^5

* Third order kinetics (cm^6 molecule^{-2} s^{-1}). Rate constants converted to second order rate constants taking the concen-

tration of H_2O into account.

As the sealed canister will contain a mixture of Ar and water vapor. it is important to assess the impact of Ar on the radiolysis of water vapor. A literature survey was performed and a few relevant papers were found (Lampe 1959, Baj et al. 1984, Jówko et al. 2001, Jonsson and Lind 1976, Mori et al. 1992, Sauer et al. 1999). In general, noble gases are used as sensitizers in radiolysis of gas mixture. In other words. radiation energy absorbed by noble gases is easily transferred to the other constituent of the gas mixture. It has also been demonstrated that energy transfer from Ar to H_2O occurs in irradiated mixtures of the two gases (Baj et al. 1984). Unfortunately, the papers found do not provide quantitative data on the energy transfer from Ar to H_2O not on the possible impact on radiation chemical yields. In addition to the energy transfer, the presence of Ar will also have an impact on the kinetics of three-body reactions occurring in the irradiated water vapor. Three-body reactions in the gas phase will become faster in the presence of Ar. This applies to reaction 1, 2, 3, 5, 10 and 15 in Table 2-2.

The rate constants for the reactions in Table 2-2 have been calculated for the three different amounts of water in the canister in the absence and presence of 1 bar (at room temperature) Ar are given in Table 2-3.

Table 2-3. Rate constants in the different systems (in $M^{-1} s^{-1}$).

Reaction number	600 g	600 g + Ar	244 g	244 g + Ar	6.7 g	6.7 g + Ar
1*	2.41E+08	5.32E+08	9.81E+07	3.88E+08	2.70E+06	2.93E+08
2*	1.26E+10	2.65E+10	4.91E+09	1.94E+10	1.35E+08	1.46E+10
3*	1.21E+09	2.65E+09	4.91E+08	1.94E+09	1.35E+07	1.46E+09
4	3.01E+10	3.01E+10	3.01E+10	3.01E+10	3.01E+10	3.01E+10
5*	4.83E+09	1.07E+10	1.96E+09	7.77E+09	5.39E+07	5.85E+09
6	6.02E+09	6.02E+09	6.02E+09	6.02E+09	6.02E+09	6.02E+09
7	6.02E−01	6.02E−01	6.02E−01	6.02E−01	6.02E−01	6.02E−01
8	1.20E+09	1.20E+09	1.20E+09	1.20E+09	1.20E+09	1.20E+09
9	2.17E+09	2.17E+09	2.17E+09	2.17E+09	2.17E+09	2.17E+09
10*	3.02E+08	6.62E+08	1.23E+08	4.85E+08	3.37E+06	3.66E+08
11	6.02E+07	6.02E+07	6.02E+07	6.02E+07	6.02E+07	6.02E+07
12	1.20E+09	1.20E+09	1.20E+09	1.20E+09	1.20E+09	1.20E+09
13	5.42E+07	5.42E+07	5.42E+07	5.42E+07	5.42E+07	5.42E+07
14	1.38E+09	1.38E+09	1.38E+09	1.38E+09	1.38E+09	1.38E+09
15*	3.26E+07	7.16E+07	1.32E+07	5.24E+07	3.64E+05	3.95E+07
16	1.81E+05	1.81E+05	1.81E+05	1.81E+05	1.81E+05	1.81E+05

* Denotes three-body reactions.

3 Numerical simulations

The numerical simulations are performed using MAKSIMA-CHEMIST (Carver et al. 1979). The conditions of the system and the corresponding input parameters are listed in Table 3-1.

Table 3-1. System and input parameters used in the numerical simulations.

System parameter	Input parameter	Comment
Water content: 600 g/m^3	$[H_2O]_0 = 3.33 \times 10^{-2}$ M	
Dose rate (Håkansson 2000): 0.5 Gy s^{-1*}	1.87×10^{15} eV L^{-1} s^{-1}	In MAKSIMA-CHEMIST the dose rate is given as energy per L rather than per kg. The conversion is based on the density of the medium (in this case the density of water vapor in the canister). The dose rate is calculated fo a distance of 0.1 m from the fuel surface.
G-values	G-values after charge neutralization from Table 2-1	In molecules/100 eV
Reactions and rate constants	Table 2-2 and 2-3	In M^{-1} s^{-1} for second order kinetics
H$_2$ content: Maximum 10 %	$[H_2]_0 = 3.33 \times 10^{-7} - 3.33 \times 10^{-3}$ M	
Time	The maximum time of the simulations was set to 1.0×10^9 s (= 31.7 years)	For longer times it would be very unrealistic to use the same dose rate and a significant fraction of the water vapor would also have been consumed.

* As reference dose rate 30 years old BWR fuel with a burnup of 55 MWd/kg is used.

As the purpose of this study was to investigate the impact of H$_2$ on the radiolytic production of corrosive species, the main focus was to monitor the influence of H$_2$ on the concentrations of the molecular oxidants O$_2$ and H$_2$O$_2$.

As temperature dependent G-values and rate constants are currently not available, the simulations do not strictly reflect the conditions prevailing in the canister. However, the general trends are assumed to be reproduced by the simulations.

4 Results and discussion

The simulations clearly show that the concentrations of the molecular oxidants O_2 and H_2O_2 increase more or less linearly with irradiation time in a system where only the reactions given in Table 2-2 are included (Figure 4-1). In reality, O_2 and H_2O_2 would have been consumed in reactions with the canister material and possibly also with the fuel cladding. However, such reactions were not included due to the time constraints of this project. The simulations clearly show that the radiolysis of water vapor will create a potentially corrosive environment. It is also clear that without any reactions allowing for water to be re-formed from O_2 and H_2O_2, the water content of the canister will start to be significantly reduced when exceeding the exposure time used in the simulations at the dose rate used in the simulations.
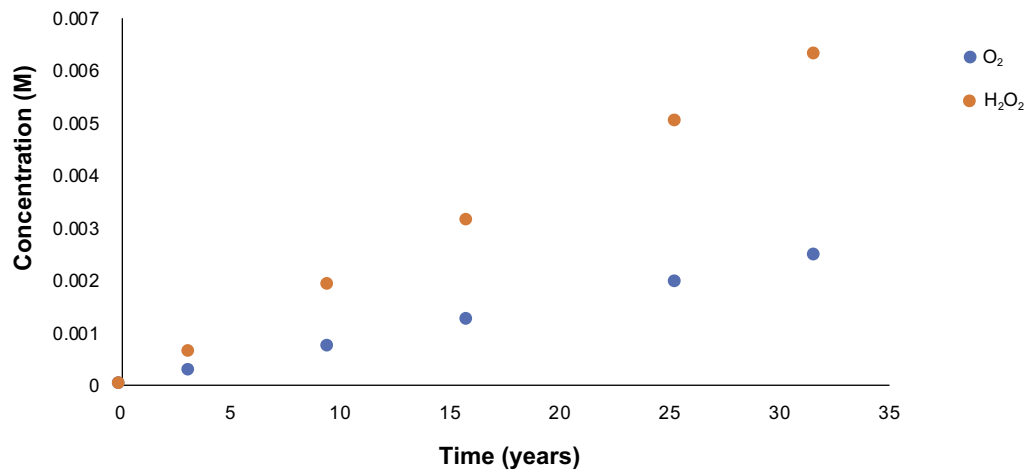

Figure 4-1. *Concentrations of O_2 and H_2O_2 as a function of irradiation time for pure water vapor.*

To investigate the impact of initial concentrations of H_2 on the production of molecular oxidants, simulations with initial H_2 concentrations ranging from 0.001 to 10 % (with respect to the molar water content) were performed. The simulations revealed quite a dramatic effect which is illustrated by the final concentrations of the molecular oxidants after 31.7 years at different initial H_2 concentrations presented in Table 4-1.

Table 4-1. Final concentrations of O_2 and H_2O_2 for different initial H_2-concentrations.

H_2 (%)	$[O_2]$ (31.7 years)/M	$[H_2O_2]$ (31.7 years)/M
0	2.5×10^{-3}	6.3×10^{-3}
0.001	2.5×10^{-3}	6.3×10^{-3}
0.01	3.1×10^{-16}	3.6×10^{-18}
0.1	2.6×10^{-16}	3.0×10^{-18}
1	7.3×10^{-17}	8.6×10^{-19}
10	2.3×10^{-18}	2.7×10^{-20}

From the table we can clearly see that an initial H_2 concentration of 0.01 % is sufficient to effectively prevent the build-up of molecular oxidants in the system under the present conditions. It is important to note the dose rate as well as the inclusion of other reactions consuming the molecular oxidants may have an impact on the minimum H_2 concentration necessary to prevent overall corrosive conditions.

The results presented above lead to the conclusion that direct corrosion of iron by water vapor will create an atmosphere where radiation induced corrosion is strongly inhibited.

To assess the impact of the amount of water vapor, the presence of Ar, the impact of H_2 and the possible energy transfer from Ar to H_2O, 54 individual simulations were performed. In the absence of a quantitative relationship describing the energy transfer from Ar to H_2O, simulations assuming 100 % energy transfer were performed. The energy transfer is handled by adding up the contributions from Ar and H_2O when calculating the density of the gas and them assuming that all the absorbed radiation energy contributes to water vapor radiolysis. Possible effects on the radiation chemical yields are not accounted for. This should be seen as a maximum effect. In the following three tables (4-2 to 4-4), the concentrations of O_2 and H_2O_2 after ca 32 years are given for pure water vapor, a mixture of water vapor and Ar taking energy transfer into account and a mixture of water vapor and Ar not taking energy transfer into account. Each table represents one amount of H_2O.

Table 4-2. Simulation results (after 31.7 years) for 6.7 g H_2O.

H_2 (M)	6.7 g H_2O (3.7×10^{-4} M)		6.7 g H_2O + Ar		6.7 g H_2O + Ar No energy transfer	
	$[O_2]$/M	$[H_2O_2]$/M	$[O_2]$/M	$[H_2O_2]$/M	$[O_2]$/M	$[H_2O_2]$/M
0	1×10^{-4}	5×10^{-6}	$6 \times 10^{-5*}$	$1.8 \times 10^{-4*}$	2×10^{-5}	7×10^{-5}
3.3×10^{-3}	3×10^{-20}	4×10^{-26}	7×10^{-18}	1×10^{-19}	3×10^{-21}	5×10^{-23}
3.3×10^{-4}	3×10^{-18}	4×10^{-24}	9×10^{-17}	2×10^{-18}	3×10^{-19}	5×10^{-21}
3.3×10^{-5}	2×10^{-16}	4×10^{-22}	2×10^{-16}	3×10^{-18}	2×10^{-17}	4×10^{-19}
3.3×10^{-6}	7×10^{-15}	1×10^{-20}	2×10^{-16}	3×10^{-18}	7×10^{-16}	1×10^{-17}
3.3×10^{-7}	2×10^{-14}	4×10^{-20}	$6 \times 10^{-5*}$	$1.8 \times 10^{-4*}$	2×10^{-15}	4×10^{-17}

* Under these conditions all H_2O has been consumed after ca 10^7 s and the oxidant concentrations refer to this point.

Table 4-3. Simulation results (after 31.7 years) for 244 g H$_2$O.

H$_2$ (M)	244 g H$_2$O (1.4 x 10^{-2} M)		244 g H$_2$O + Ar		244 g H$_2$O + Ar No energy transfer	
	[O$_2$]/M	[H$_2$O$_2$]/M	[O$_2$]/M	[H$_2$O$_2$]/M	[O$_2$]/M	[H$_2$O$_2$]/M
0	2 x 10^{-3}	2 x 10^{-3}	6 x 10^{-3}	2 x 10^{-2}	7 x 10^{-4}	3 x 10^{-3}
3.3 x 10^{-3}	1 x 10^{-18}	2 x 10^{-21}	7 x 10^{-18}	2 x 10^{-19}	5 x 10^{-19}	2 x 10^{-20}
3.3 x 10^{-4}	6 x 10^{-17}	1 x 10^{-19}	8 x 10^{-17}	2 x 10^{-18}	3 x 10^{-17}	9 x 10^{-19}
3.3 x 10^{-5}	5 x 10^{-16}	9 x 10^{-19}	1 x 10^{-16}	4 x 10^{-18}	2 x 10^{-16}	7 x 10^{-18}
3.3 x 10^{-6}	7 x 10^{-16}	1 x 10^{-18}	1 x 10^{-16}	4 x 10^{-18}	4 x 10^{-16}	1 x 10^{-17}
3.3 x 10^{-7}	2 x 10^{-3}	2 x 10^{-3}	6 x 10^{-3}	2 x 10^{-2}	7 x 10^{-4}	3 x 10^{-3}

Table 4-4. Simulation results (after 31.7 years) for 600 g H$_2$O.

H$_2$ (M)	600 g H$_2$O (3.3 x 10^{-2} M)		600 g H$_2$O + Ar		600 g H$_2$O + Ar No energy transfer	
	[O$_2$]/M	[H$_2$O$_2$]/M	[O$_2$]/M	[H$_2$O$_2$]/M	[O$_2$]/M	[H$_2$O$_2$]/M
0	2 x 10^{-3}	6 x 10^{-3}	5 x 10^{-3}	3 x 10^{-2}	1 x 10^{-3}	7 x 10^{-3}
3.3 x 10^{-3}	2 x 10^{-18}	3 x 10^{-20}	8 x 10^{-18}	4 x 10^{-19}	2 x 10^{-18}	9 x 10^{-20}
3.3 x 10^{-4}	7 x 10^{-17}	9 x 10^{-19}	7 x 10^{-17}	4 x 10^{-18}	5 x 10^{-17}	3 x 10^{-18}
3.3 x 10^{-5}	3 x 10^{-16}	3 x 10^{-18}	1 x 10^{-16}	6 x 10^{-18}	2 x 10^{-16}	1 x 10^{-17}
3.3 x 10^{-6}	3 x 10^{-16}	4 x 10^{-18}	1 x 10^{-16}	6 x 10^{-18}	2 x 10^{-16}	1 x 10^{-17}
3.3 x 10^{-7}	2 x 10^{-3}	6 x 10^{-3}	5 x 10^{-3}	3 x 10^{-2}	1 x 10^{-3}	7 x 10^{-3}

From the tables above we can clearly see that the oxidant concentrations increase with increasing water content. It is also clear that, for each water content, the oxidant concentrations increase in the presence of Ar taking energy transfer into account. The impact of Ar is highest for the lowest water content which is to be expected. The kinetic effect of Ar (i.e., in three body collisions) is relatively small for all amounts of H$_2$O. The simulations performed at different H$_2$ concentrations show that H$_2$ has a very strong effect on the production of oxidants. For the lowest amount of water, it is obvious that all H$_2$ concentrations used in the simulations are sufficient to completely inhibit significant oxidant production (except when taking the energy transfer from Ar into account which leads to complete consumption of water after around 10^7 s). For the two larger amounts of water, the lowest H$_2$ concentration (3.3 × 10^{-7} M) has no effect on the oxidant production. As a general conclusion from the somewhat limited data set presented above, oxidant production and thereby corrosion is inhibited by H$_2$ at 0.1 % H$_2$ (compared to the amount of water) and above.

References

SKB's (Svensk Kärnbränslehantering AB) publications can be found at www.skb.com/publications.

Baj H, Symanowicz M, Jówko A, 1984. The rare gas sensitized radiolysis of hydrogen chloride. Radiation Physics and Chemistry 23, 537–543.

Carver M B, Hanley D V, Chaplin K R, 1979. MAKSIMA-CHEMIST: a Program for Mass Action Kinetics Simulation by Automatic Chemical Equation Manipulation and Integration Using Stiff Techniques. Report AECL—6413, Atomic Energy of Canada Limited.

Dixon R S, 1970. Dissociation of water vapour by photolitic, radiolytic, and electron impact methods. Radiation Research Reviews 2, 237–296.

Håkansson R, 2000. Beräkning av nuklidinnehåll, resteffekt, aktivitet samt doshastighet för utbränt kärnbränsle. SKB R-99-74, Svensk Kärnbränslehantering AB. (In Swedish.)

Jonsson B-Ö, Lind J, 1976. Comparative charge-exchange mass spectrometric and argon-sensitized radiolytic studies of methanol. Journal of the Chemical Society, Faraday Transactions 2, 72, 906–912.

Jówko A, Wnorowski K, Kowalczyk J, Wojciechowski K, 2001. Kinetics of OH formation in pulse radiolysis of Ar-H_2O gaseous mixtures. Radiation Physics and Chemistry 61, 27–34.

Lampe F W, 1959. The direct radiolysis and the radiation-sensitized hydrogenation of ethylene. Radiation Research 10, 691–701.

Mori T, Kanou K, Ishikawa Y-I, Arai S, 1992. Formation of highly excited oxygen atoms $O(2p^3 3p, {}^5P)$ and $O(2p^3 3s, {}^5S)$ in electron irradiation of mixtures of rare gases and O_2. The Journal of Chemical Physics 96, 8258–8266.

Pastina B, LaVerne J A, 2001. Effect of molecular hydrogen on hydrogen peroxide in water radiolysis. The Journal of Physical Chemistry A 105, 9316–9322.

Sauer C G, Barnes I, Becker K H, Geiger H, Wallington T J, Christensen L K, Platz J, Nielsen O J, 1999. Atmospheric chemistry of 1,3-dioxolane: kinetic, mechanistic and modelling study of OH radical initiated oxidation. The Journal of Physical Chemistry A 103, 5959–5966.

SKB, 2010. Design, production and initial state of the canister. SKB TR-10-14, Svensk Kärnbränslehantering AB.

Trummer M, Jonsson M, 2010. Resolving the H_2 effect on radiation induced dissolution of UO_2-based nuclear fuel. Journal of Nuclear Materials 396, 163–169.

Willis C, Boyd A W, 1976. Excitation in the radiation chemistry of inorganic gases. International Journal for Radiation Physics and Chemistry 8, 71–111.

SKB is responsible for managing spent nuclear fuel and radioactive waste produced by the Swedish nuclear power plants such that man and the environment are protected in the near and distant future.

skb.se